Interactive Visualization Techniques
for Neurosurgery Planning

Stefan Diepenbrock[†1], Jörg-Stefan Praßni[1], Florian Lindemann[1], Hans-Werner Bothe[2], Timo Ropinski[1]

[1] University of Münster, [2] University Hospital Münster

Abstract

We present concepts for pre-operative planning of brain tumor resections. The proposed system uses a combination of traditional and novel visualization techniques rendered in real-time on modern GPUs in order to support neurosurgeons during intervention planning. A set of multimodal 2D and 3D renderings conveys the relation between the lesion and the various structures at risk and also depicts data uncertainty. To facilitate efficient interactions while providing a comprehensible visualization, all employed views are linked. Furthermore, the system allows the surgeon to interactively define the access path by clicking in the 3D views as well as to perform distance measurements in 2D and 3D.

Categories and Subject Descriptors (according to ACM CCS): I.3.7 [Computer Graphics]: Picture/Image Generation—Three-Dimensional Graphics and Realism

1. Introduction

We propose an application prototype for neurosurgical planning that supports a large variety of modalities (fMRI, DTI, T1 pre, T1 post, T2, FLAIR, SWI, CT). Our application integrates proven solutions as 2D slice rendering with state of the art techniques and some novel approaches, into a workflow leading towards finding an optimal access path for neurosurgery. Our focus are computer graphics techniques utilized to enable these visualizations, including multimodal volume raycasting with enhanced shading techniques for brain rendering, two novel projection techniques, enhanced lift charts and uncertainty visualization techniques for DTI and fMRI. We will also discuss the feedback received from domain experts, who evaluated the clinical value of the proposed application.

2. Workflow

In cooperation with our medical partner, we have identified two main steps for the pre-operative planning workflow.
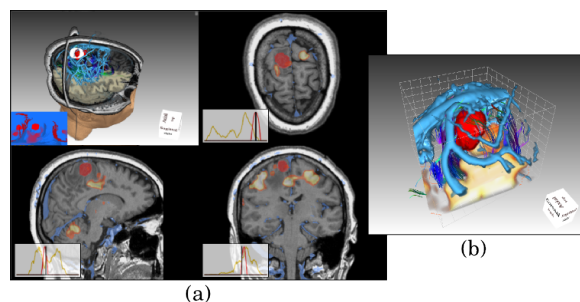

Figure 1: *Exploring the data and planning an initial access path can be done by exploiting multimodal 3D and 2D views (a). Furthermore, the tumor view allows a close-up inspection of the vicinity of the resection region (b).* (**Workflow Step 1**)

First, the initial investigation of the data in combination with an interactive access path specification. Second, the deeper analysis of the chosen access path and the actual preparation for the surgery. Figures 1 and 2 show the views exploited in workflow step 1 and workflow step 2. During the planning, the surgeon can always go back from step 2 to step 1 in order to choose an entirely new access path.
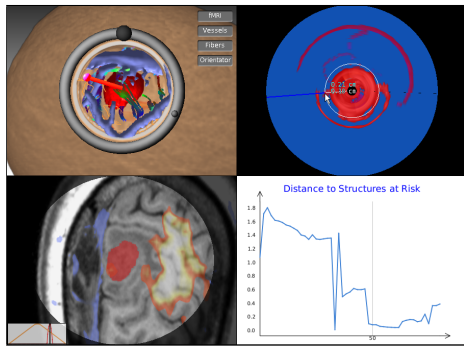
† {diepenbrock,j-s.prassni,f_lind03,hwbothe,timo.ropinski}@uni-muenster.de

Figure 2: *In-detail inspection as well as modification of the access path and operation preparation by exploiting a probe view, a cylindrical access path projection, a surgeon microscope slice view and an access path distance plot. (**Workflow Step 2**)*

As can be seen in Figure 1 (a), in the first step we combine classical 2D slice views with a 3D context view that integrates relevant information from the available modalities. The 2D slice views provide insight into structures and allow the neurosurgeon to identify structures inside the tumor and diagnose its type. The location of the tumor as well as its relation to risk structures is depicted in the 3D view, which is further overlaid with a tumor map showing a projection of relevant structures as seen from the tumor. As shown in Figure 1 (b), an additional close-up view of the tumor and the relevant adjacent structures is available to identify vessels and fibers that may be infiltrated or displaced by the tumor. Using these views the neurosurgeon can place one or more access paths before analyzing and comparing them in step 2.

In the second step (see Figure 2) we exploit a classical probe view (top left), which shows all structures inside the access path and provides a preview of how the access path would look like during operation. It also enables the surgeon to fine tune the previously chosen access path. To locate structures close to the access path the top right view displays a projection of the structures surrounding the access path onto the surface of the access path cylinder. A plot showing the minimum distances of relevant structures along the access path is located at the bottom right to allow an easy comparison of several possible paths. Finally, in the bottom left the system offers a slice view that is centered around the access path and oriented perpendicular to it, thereby providing a view corresponding to the operation microscope focusing at a certain depth. In the following we will discuss the preprocessing, visualization and interaction techniques we employed and give a short evaluation based on the feedback we received from neurosurgeons.
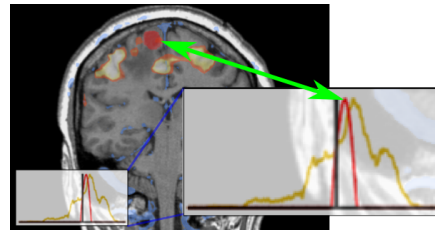

Figure 3: *Enhanced lift charts indicate the current position in the slice stack and display the amount of malignant tissue (red) as well as fMRI signal (yellow).*

3. Uncertainty Extraction

To deal with the uncertainty introduced through DTI, we incorporate the fiber context as well as the fiber anisotropy. Since DTI is less certain in regions near bone or air, we have applied a volume analysis that first applies a masking in order to extract bone and air structures. Based on this masking volume we perform a distance transformation that computes the distance d to these structures for each fiber segment. Thus, a user-defined security margin can be defined around air and bone structures. We normalize the computed distance to obtain a structure uncertainty U_S. To get the final uncertainty for a fiber segment, we combine U_S with the anisotropy uncertainty U_A, to obtain the overall uncertainty $U = max(U_S, U_A)$.

4. Visualization

2D and 3D Views. The 2D slice views integrated into our system are standard slice views, which have been extended by using enhanced lift charts [TMS*06]. To quickly identify the most important structures, we overlay one chosen modality with the tumor segmentation mask, the fMRI signal and the vessels. Within the lift charts (see Figure 3), we depict for each slice the extent of malignant tissue (red curve) as well as the fMRI signal (yellow curve). The current slice in the stack is also indicated to help the user to navigate through the slices.

To generate high-quality 3D views, we exploit GPU-based volume ray-casting [KW03], which has been shown [SHC*09] to generate images superior to other volume rendering techniques. Our multi volume raycaster is inspired by the approach presented by Lindholm et al. [LLHY09]. In order to integrate the fiber geometry into the 3D views, we have modified the exit points used by our GPU-based raycaster, as proposed by Scharsach [Sch05] (see Figure 4).

Because gradients in MRI scans are unreliable due to noise, we use a distance based darkening (*dark means deep*) and depth darkening [LCD06] to render the brain and simulate the effects of a global illumination model with a minimal performance impact. We render the brain without shading (see Figure 5 (b)) and then apply the depth darkening to
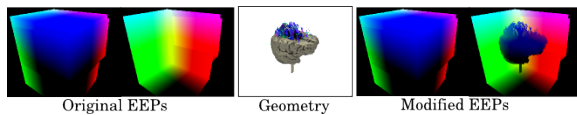
Figure 4: *Integration of geometry and single volume raycasting results into the EEPs of our multi volume raycaster.*

(a)   (b)   (c)

Figure 5: *Comparing different techniques to shade the brain (using the same transfer-function): Gradient based shading (a), no shading (b), depth darkening and dark means deep (c).*

the image. The resulting image depicts the structures of the brain more comprehensible manner (compare Figure 5 (a) and (c)). We then integrate the rendering of the brain into our multi volume raycasting using the EEP modification technique we employed for geometry integration (see Figure 4).

There are three different 3D views provided by our system. The 3D *context view*, shown during the first step of the workflow, integrates all relevant modalities into a comprehensible rendering. It can be used to identify the various structures at risk and understand how they relate and interact with each other. To prevent cluttering, all modalities can be easily deactivated through on-screen buttons (see Figure 1 (top right)). Additionally, the user can specify a region of interest based on the distance to the tumor surface for the vessel volume. Moreover, the 3D context view allows the surgeon to efficiently define the access path by using the mouse. After the access path has been defined, a 3D *probe view* is exploited during the second step of the workflow in order to identify all related risk-structures lying along the chosen path. This probe view allows the physician to see the access path in a similar way as during the resection. Furthermore, the surgeon may use the ring widget (see Figure 2 (top left)) to rotate the head around the fixed access path axis in order to simulate the possible orientations during the resection. The bigger ring marker can be used as rotation widget, while the smaller one indicates the direction pointing to the patient's nose.

The third 3D view is the *tumor view*, which focusses on the spatial relation between the tumor and nearby structures at risk. As the context view, it also integrates all relevant modalities, but displays a close-up showing only the tumor and structures in the proximity of the tumor. Thus, the tumor view can be used to support the surgeon when analyzing how close the tumor is to vital functional areas. The surgeon can especially analyze which fibers infiltrate the tumor to what extent, or which fibers are displaced.

4.1. Projection Techniques

To provide informative views of the structures at risk, we exploit two projection techniques. One, showing the structures close to the tumor and one showing the structures close to the access path. For both projection techniques we employ a red-blue color mapping, where structures at risk nearby are displayed in red. Using a volume raycaster these projec-
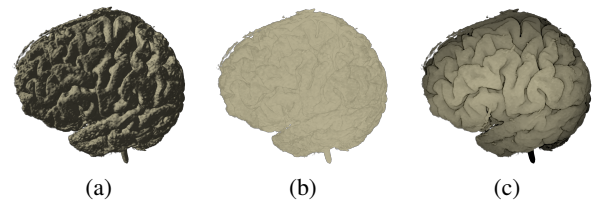
tions can calculated by simply passing spherical/cylindrical Entry-Exit-Points (EEPs) to the raycaster (see Figure 6). Because OpenGL does not allow for easy spherical/cylindrical projections we use an OpenCL kernel to raytrace the Proxy-Geometry of one or multiple volumes and generate these EEPs.

Tumor Map. The *tumor map*, which is overlaid on the 3D context view, is inspired by the projection type presented by Rieder et al. [RWS*10]. The tumor map provides all necessary information that is required to identify the target location of the access path, which can be done by clicking on the tumor map. Distances to structures at risk, such as vital functional areas or the pyramidal tract, can easily be measured by moving the mouse over the tumor map. The measured distances are also displayed in the context view (see Figure 2 (top left)). We generate the map by performing two spherical raycastings from the center of the tumor. First, we render the tumor mask using an inverted transfer function (i.e., the inside of the tumor is transparent, the rest is opaque). We then use the first-hit points as entry points for a second raycasting of all risk-structures. By calculating the distance between entry- and first-hit points for this raycasting we get a distance map to which we apply a red-blue color mapping.

Access Path Projection. Besides their distance to the tumor, the distance of structures at risk to the access path is also important. Therefore, the *access path projection* shows the distance to all relevant structures as seen from the access path (see Figure 7 (right)). The result of this cylindrical projection is mapped to a disc that is rendered in a view, which is linked to the probe view. The center of the projection represents the deeper end of the access path. As with the tumor map, moving the mouse cursor over a red region of the map will automatically measure the distance to the structure at risk and display it in the probe view (see Figure 7 (left)). For the access path projection we also display the distance along the access path, which is an important information for the surgeon.

4.2. Uncertainty Visualization

DTI Uncertainty. When visualizing the DTI fiber tracts, we incorporate the derived uncertainty information intro-
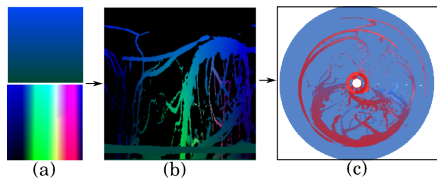
Figure 6: *Cylindrical entry- and exit points (a), result of the cylindrical raycasting (first hit points) (b), resulting distances color coded and mapped to a disc (c).*
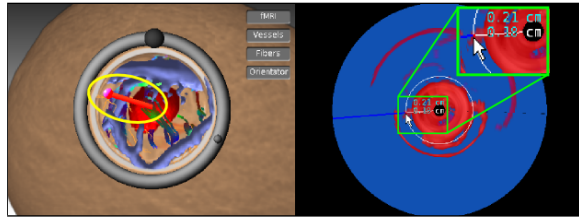

Figure 7: *Access Path Projection: The measured distances are displayed in the probe view using linking.*

duced in Subsection 3. We encode the uncertainty in the saturation and value of the displayed fiber color in the HSV color space. While we in general use the standardized directional fiber color-mapping MDs are used to, we lower the saturation and value in regions of high uncertainty (see Figure 8). Thus, uncertain fibers become less emphasized and their orientation, which can also be considered as less certain, is less prominent.

fMRI Uncertainty. To depict the uncertainty of the fMRI signal, we have applied an approach inspired by the work of Nguyen et al. [NYE*10]. We display the core of each fMRI region by exploiting a diffusely emitting light signal. Additionally, in order to express the uncertainty regarding the size of theses regions, we add an uncertainty margin, depicted by orange borders (see Figure 8). To generate this visualization we render the fMRI signal twice: In the first pass we render the core regions using a higher threshold, while in the second pass we use a lower threshold and apply an edge detection filter. We than composit this border-image with the result of the first pass.

5. Interaction Techniques

A detailed exploration of the different modalities would not be possible without exploiting sophisticated interaction techniques. Therefore, we have integrated several interaction techniques which support the mental linking of the different views as well as a deeper understanding of the data. Thus, the surgeon can measure distances in the image, specify and alter the access path and interactively navigate through all 3D views. The whole set of interaction techniques is demonstrated in the accompanying video.

6. Evaluation

Our application prototype was reviewed as an entry in the IEEE Visualization Contest 2010. Two of the five reviewers were neurosurgeons and the clinical value was rated as high (7 and 9 out of 9). We have indepedantly shown our application to several domain experts and got very positive feedback about the integration of a wide range of modalities into an intuitive 3D visualization. The enhanced lift charts were also appreciated for providing a simple indication of the current position in the slice stack.

References

[KW03] KRÜGER J., WESTERMANN R.: Acceleration techniques for GPU-based volume rendering. In *IEEE Vis* (2003), pp. 287–292. 2

[LCD06] LUFT T., COLDITZ C., DEUSSEN O.: Image enhancement by unsharp masking the depth buffer. *ACM Transactions on Graphics 25*, 3 (jul 2006), 1206–1213. 2

[LLHY09] LINDHOLM S., LJUNG P., HADWIGER M., YNNERMAN A.: Fused Multi-Volume DVR using Binary Space Partitioning. In *Computer Graphics Forum* (2009), vol. 28, John Wiley & Sons, pp. 847–854. 2

[NYE*10] NGUYEN T. K., YNNERMAN A., EKLUND A., LJUNG P., HERNELL F., OHLSSON H., ANDERSSON M., KNUTSSON H., FORSELL C.: Concurrent volume visualization of real-time fmri. In *IEEE/EG Volume Graphics* (2010). 4

[RWS*10] RIEDER C., WEIHUSEN A., SCHUMANN C., ZIDOWITZ S., PEITGEN H.-O.: Visual support for interactive post-interventional assessment of radiofrequency ablation therapy. In *EuroVis* (2010). 3

[Sch05] SCHARSACH H.: Advanced GPU raycasting. *Proceedings of CESCG 5* (2005), 67–76. 2

[SHC*09] SMELYANSKIY M., HOLMES D., CHHUGANI J., LARSON A., CARMEAN D., HANSON D., DUBEY P., AUGUSTINE K., KIM D., KYKER A., ET AL.: Mapping high-fidelity volume rendering for medical imaging to cpu, gpu and many-core architectures. *IEEE Vis* (2009), 1563–1570. 2

[TMS*06] TIETJEN C., MEYER B., SCHLECHTWEG S., PREIM B., HERTEL I., STRAUSS G.: Enhancing slice-based visuaizations of medical volume data. In *EuroVis* (2006), pp. 123–130. 2
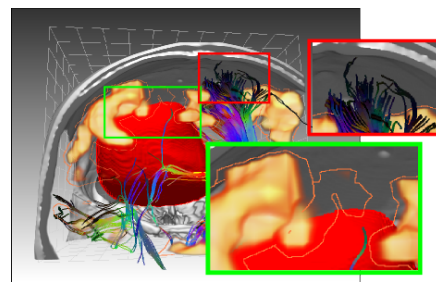
Figure 8: *Uncertainty visualization.* **fMRI (green inset):** *Core regions are rendered using a diffusely emitting light signal, uncertainty borders are rendered in orange.* **DTI (red inset):** *Fibers close to bone and air are rendered with less saturation and brightness to mark them as uncertain.*